Signal Processing: *Image Communication* 29 (2014) 1149–1157

Contents lists available at ScienceDirect

Signal Processing: *Image Communication*

journal homepage: www.elsevier.com/locate/image

Blind image quality assessment using a reciprocal singular value curve

Qingbing Sang [a,1], Xiaojun Wu [a,*], Chaofeng Li [a], Alan C. Bovik [b]

[a] *Key Laboratory of Advanced Process Control for Light Industry (Ministry of Education), School of Internet of Things Engineering, Jiangnan University, Wuxi 214122, China*

[b] *Laboratory for Image and Video Engineering (LIVE), The University of Texas at Austin, Austin, TX 78712, USA*

ARTICLE INFO

Article history:
Received 1 November 2013
Received in revised form
12 September 2014
Accepted 17 September 2014
Available online 28 September 2014

Keywords:
Image quality assessment
Singular value decomposition (SVD)
Reciprocal singular value curve
No-Reference

ABSTRACT

The reciprocal singular value curves of natural images resemble inverse power functions. The bending degree of the reciprocal singular value curve varies with distortion type and severity. We describe two new general blind image quality assessment (IQA) indices that respectively use the area and curvature of image reciprocal singular value curves. These two methods almost require very little prior knowledge of any image or distortion nor any process of training, and they can handle multiple unknown distortions, hence they are no-training methods. Experimental results on five simulated databases show that the proposed algorithms deliver quality predictions that have high correlation with human subjective judgments, and that are competitive with other blind IQA models.

1. Introduction

An increasingly large number of digital images are being produced by professional and casual users as digital cameras have become ubiquitous in smartphones, tablets, and stand-alone units. Since in nearly every instance it is desirable to produce clear, crisp images free of excessive noise, annoying blur or other artifacts, the development of methods for automatically assessing the perceptual quality of digitally acquired images has become an important goal of model and algorithm developers [1]. Such tools would greatly facilitate the sorting and culling of the large volumes of images that are so easily obtained. Current objective image quality assessment (IQA) methods fall into three general categories: Full Reference (FR), Reduced Reference (RR) and No Reference (NR) or Blind [2]. FR and RR models require that all or part of the information about the reference image be available. However, in most application scenarios information regarding a reference image is inaccessible. Hence effective NR models may ultimately prove to be more viable.

Existing NR IQA models can be roughly divided into two categories: distortion-specific and general purpose. Distortion-specific models are specialized for a single type of distortion, for example, [3–6] are designed to assess blur distortion, while [7,8] are dedicated to measuring the perceptual severity of JP2K distortions. These models are effective in specific settings. By contrast, general purpose models are intended to handle multiple, possibly unknown distortions.

In recent years, several general purpose NR IQA algorithms have been proposed. These models can further be subdivided into two categories. State-of-the-art learning-based general purpose NR IQA algorithms include GRNN [9], DIIVINE [10], CORNIA [11], BLIINDS-II [12] and BRISQUE [13]. Using a neural network, the authors of [9] proposed a novel NR IQA algorithm that was trained on the local mean, entropy and gradient extracted from the distorted image as well as its phase congruency (PC) map. Based on perceptually

* Corresponding author.
E-mail addresses: sangqb@163.com (Q. Sang), xiaojun_wu_jnu@163.com (X. Wu), bovik@ece.utexas.edu (A.C. Bovik).
[1] Tel.: +86 13812267640.

http://dx.doi.org/10.1016/j.image.2014.09.005
0923-5965/

relevant natural scene statistics (NSS) models, the authors of [10] first proposed a new two-step framework named blind image quality index (BIQI) [14], then later refined these to create the Distortion Identification-based Image Verity and Integrity Evaluation (DIIVINE) index. The authors of [11] present an efficient unsupervised NR IQA framework. They use raw image patches extracted from a set of unlabeled images to learn a dictionary in an unsupervised manner. BLIINDS-II [12] introduces a generalized parametric model of the natural statistics of local image discrete cosine transform (DCT) coefficients to predict image quality scores. The BRISQUE model [13] deploys a space-domain NSS model from
which quality-predictive features are derived. The above-mentioned NR IQA algorithms are generally based on machine learning principles, and hence require conducting training on and testing against human opinion scores of distorted images. Of course, learning-based models can only reliably assess quality degradations arising from the distortion types that they have been trained on, potentially limiting their utility. In many practical situations there is no available information of new or varying distortions, hence it is highly desirable to create algorithms that reduce or eliminate this dependence.

In order to overcome the disadvantages of learning based IQA methods, a number of unsupervised, training free NR IQA models have been proposed. In [15], the authors proposed an NR IQA model that operates by seeking latent quality factors. A newer IQA model, called the natural image quality evaluator (NIQE) [16] is based on the construction of a "quality aware" collection of perceptually relevant statistical gradient and phase congruency features based on a simple and successful space domain NSS model. This model does require a corpus of pristine images from which to estimate the model parameters. In [17] the authors proposed a quality-aware clustering (QAC) method which learns a set of centroids at each quality level. This method does not require human Mean Opinion Scores (MOS), but it does require distorted images to learn from. In [18], the authors proposed a no-training method which using a simple functional relationship of perceptually relevant image features to predict image quality. The limitation of the algorithm is that a classification algorithm is needed to distinguish noise distortion from other distortion categories. Here we develop an alternative general purpose NR IQA algorithm that also is able to predict the perceptual severities of multiple kinds of distortions without any training on human scores. This new 'completely blind' IQA model uses very simple features derived from a 'reciprocal singular value curve' computed from the image. The new model is tested on five IQA databases and is shown to deliver highly competitive performance against other NR IQA models and even against widely-used FR IQA algorithms.

The rest of the paper is organized as follows. Section II analyzes the relationship between image quality and the reciprocal singular value curve. Section III presents the framework of the new image quality model. Experiments conducted on five public IQA databases are presented and analyzed in Section IV. Section V concludes the paper.

2. Relationship between image quality and singular values

2.1. A. Brief review of singular value decomposition

Every gray scale image can be considered to be a matrix. Any $m \times n$ real matrix A can be decomposed into a product of three matrices, i.e., $A = USV^T$, where U and V are orthogonal matrices, $U^TU = V^TV = I$ and $S = \begin{bmatrix} S_r & 0 \\ 0 & 0 \end{bmatrix}$, where $S_r = diag(\sigma_1, \sigma_2, \ldots, \sigma_r), S_1 = (\sigma_1, \sigma_2, \ldots, \sigma_r)$, where r is the rank of A. The diagonal entries of S are the singular values of A, the columns of U are the left singular vectors of A, and the columns of V are called the right singular vectors of A. This decomposition is the Singular Value Decomposition (SVD) of A. This useful tool of linear algebra has been applied to numerous image processing problems including image denoising, compression, watermarking, etc.

The singular value decomposition (SVD) has previously been successfully applied to the FR IQA problem. Existing FR IQA methods that use SVD can be divided into two categories. The first uses only the first singular value to assess image quality. For example, the MSVD algorithm proposed in [19] uses the degree of change of the singular value of the distorted image relative to the singular value of the reference image as the image quality evaluation criteria. The second category also uses the left and right singular vectors to assess image quality [20]. Here we conduct a more detailed study of the behavior of singular values on distorted images and use this to develop an NR IQA model. We find that a simple 'reciprocal singular value curve' supplies adequate 'distortion aware' information to construct a blind image quality assessment model.

2.2. B. Image quality analysis using a reciprocal singular value curve

In order to demonstrate the relationship between image distortion and singular values, we arbitrarily selected a source image and four blurred versions of it from the CSIQ database [21], as shown in Fig. 1. The images are displayed by order of blur degree. The singular value decomposition was applied to each of the blurred images yielding singular vectors from each. The singular values are plotted against the index of the singular vector for each image, as depicted in Fig. 2. Similarly, we selected another source image and for each of four different distortion types, produced four distorted images suffering from different degrees of distortion. The four distortions are JPEG, JP2K, additive white Gaussian noise and a contrast artifact. We applied the singular value decomposition for each, producing the corresponding singular curves shown in Fig. 3.

From Figs. 2 and 3, it may be observed that the slope of the curve becomes increasingly gentle with larger degrees of distortion with the exception of additive noise. We have observed this behavior over all of the images we have tested. The shape of the curve can be accurately fitted by

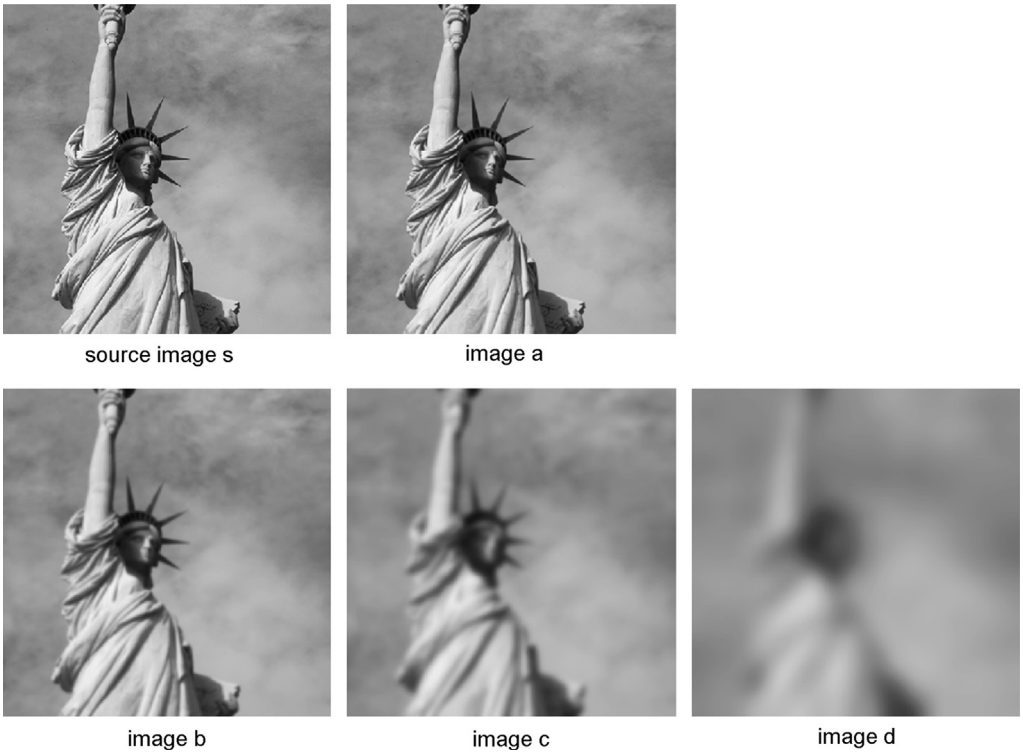

Fig. 1. Source image s and four blurred versions of it. Degree of blur increases from a to d.

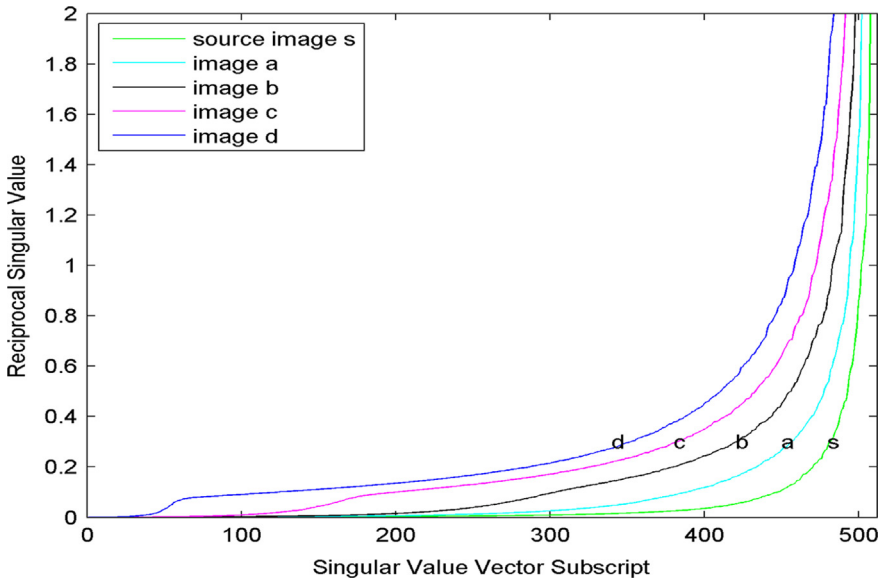

Fig. 2. Reciprocal singular value curves of the images in Fig. 1.

an inverse power function $y=(r-x)^{-q}$, where y is the reciprocal singular value, x is the corresponding subscript of y in the singular value vector and r is the number of the singular values. Since the rate of fall-off of the reciprocal singular value curve characterizes the degree of distortion, it has the potential to serve as a reliable indicator of image quality.

3. A blind image quality index using the singular value

The simulated reciprocal singular value curves of two different hypothetical distorted images are shown in Fig. 4, where $S1$ and $S2$ are the areas enclosed by their respective reciprocal singular value curves, and $q1$ and $q2$ are the exponents of the two curves. In the following, we will

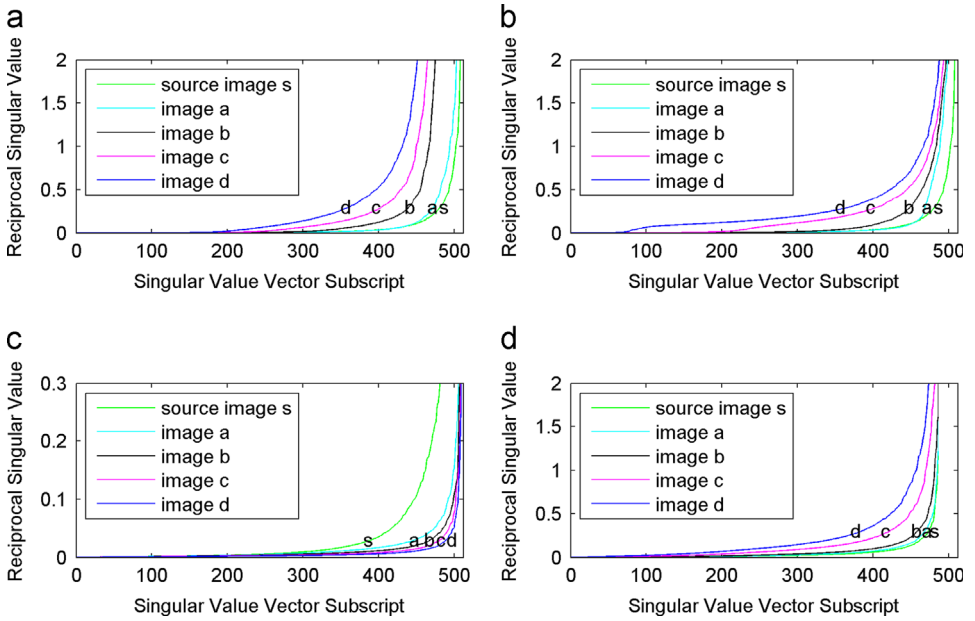

Fig. 3. Reciprocal Singular Values Curves of an image impaired by different types of artifacts. (a) JPEG, (b) JP2K, (c) noise, and (d) contrast.

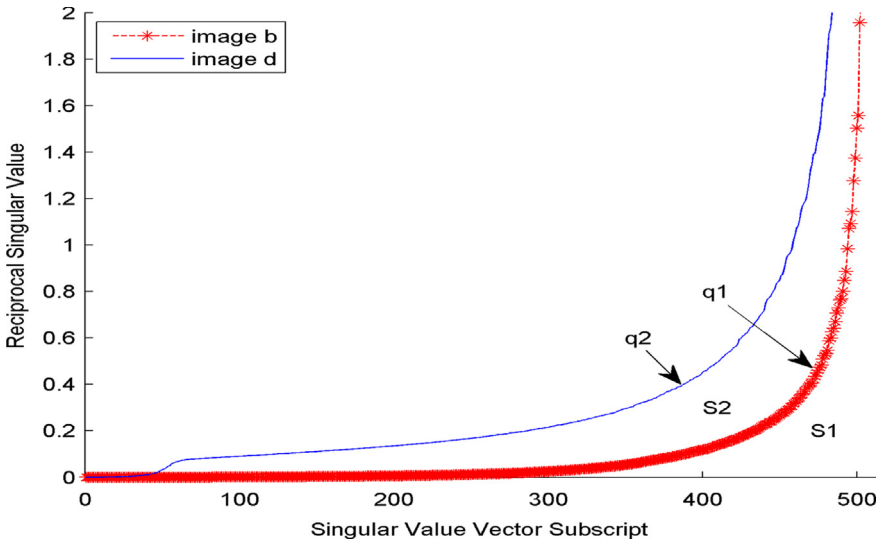

Fig. 4. Reciprocal singular value curves of two hypothetical distorted images.

design and construct two blind image quality indices using measurements of area and curvature of best-fit curves to distorted image singular value vectors.

3.1. A. Quality prediction using the area of the reciprocal singular value curve

The reciprocal singular value curve is a function $y = 1/S_1(i)$, where S_1 is the singular value vector. The area of S may be estimated by the following formula (1).

$$S = \int_0^r f(i)di = \int_0^1 f(i)di + \int_1^2 f(i)di + \cdots + \int_{r-1}^r f(i)di \approx \sum_{i=1}^{r} \left(\frac{1}{S_1(i)}\right) \quad (1)$$

where r is the number of singular values, and S_1 is the singular value vector.

In order to eliminate the influence of the image size, we use the average area to represent image quality, and then define a blind image quality index:

$$Q_{area} = \frac{\sum_{i=1}^{r} (1/S_1(i))}{r}, S_1(i) > \alpha \quad (2)$$

where α is a threshold value. Since the shapes of reciprocal singular value curves are different for different distorted

categories as, shown in Fig. 3, a threshold value is needed when measuring different distortion types.

3.2. B. Quality prediction using the exponent of reciprocal singular value curve

As mentioned before, the shape of the singular value curve resembles an inverse power function, which can be modeled as $y=(r-i)^{-q}$. In the approximation function, q dictates the exponential fall-off of the reciprocal singular value curve, which corresponds to the severity of image distortion. Hence we use measured values of q to predict image quality. Taking logarithms yields

$$\ln(y^{-1}) = q\ln(r-i) \tag{3}$$

Let $Y=\ln(y^{-1}), X=\ln(r-i)$

$$\text{then} \quad Y = qX \tag{4}$$

which is linear in q. Linear regression can be used to find q. We use least squares to minimize the residual sum of squares:

$$\min \quad Z=\sum_{i=1}^{r} e_i^2 = \sum_{i=1}^{r} (Y_i - qX_i)^2 \tag{5}$$

Equating the derivative of (5) to zero gives

$$\frac{\partial Z}{\partial q} = \sum_{i=1}^{r} 2(Y_i - qX_i)(-X_i) = 0 \tag{6}$$

with solution

$$q = \frac{\sum_{i=1}^{r} X_i Y_i}{\sum_{i=1}^{r} X_i^2} \tag{7}$$

or

$$q = \frac{\sum_{i=1}^{r} \ln(r-i)\ln(S1(i))}{\sum_{i=1}^{r} \ln(r-i)\ln(r-i)} \tag{8}$$

From Fig. 4, it may be observed that when the singular value is very small, the reciprocal singular value curves of different images do not differ much, which leads to a loss of discrimination power, so only larger singular values are used to distinguish differences in image quality. We impose a threshold β to remove small singular values. Then define the second image quality index as

$$Q_{exponent} = \frac{\sum_{i=1}^{r} \ln(r-i)\ln(S1(i))}{\sum_{i=1}^{r} \ln(r-i)\ln(r-i)}, \text{where } S1(i) > \beta \tag{9}$$

where S_1 is the singular value vector, and r is the number of singular values. The parameter β is a threshold, whose value will be discussed in the following section.

4. Performance evaluation

4.1. A. Databases and metrics for comparison

We used five publicly available image quality databases to test the models Q_{area} and $Q_{exponent}$, including CSIQ [21], LIVE2 [22], TID2008 [23], TOYAMA [24], and IVC [25]. The characteristics of these five databases are summarized in Table 1.

There are two commonly used performance metrics that are employed to evaluate the competing IQA models. The first is the Spearman Rank-Order Correlation Coefficient (SROCC), which can measure the prediction monotonicity of an IQA model. This metric operates on the ranked data points and ignores the relative distances between data points. The second metric is the Pearson Linear Correlation Coefficient (CC), which is a numerical measure of the strength of a linear association between MOS and the objective scores following nonlinear regression. For the nonlinear regression, we used the following mapping function [26]:

$$Quality(x) = \beta_1(0.5 - 1/(1+\exp(\beta_2(x-\beta_3)))) + \beta_4 x + \beta_5 \tag{10}$$

4.2. B. Image blocking

It is well-known that the computational complexity of SVD is O(N^3). If the image size is large, it could be too time-

Table 1
Benchmark test databases for IQA.

Database	Source images	Distortion types	Distorted images	Observers
LIVE2	29	5	779	161
TID2008	25	17	1700	838
CSIQ	30	6	866	35
TOYAMA	14	2	168	16
IVC	10	4	185	15

Table 2
Performance (SROCC) and runtimes (s) of Q_{area} using different block size and different values of α on the CSIQ blur database.

Size	Time (s)	$\alpha=0.5$	$\alpha=3$	$\alpha=7$	$\alpha=11$	$\alpha=15$	$\alpha=19$
16×16	48.6	0.8724	0.9204	0.8898	0.8502	0.8284	0.8086
32×32	24.2	0.8998	0.8827	0.9205	0.8937	0.8643	0.8452
64×64	18.0	0.9100	0.3159	**0.9312**	0.9205	0.9015	0.8853
128×128	**17.3**	0.9070	0.8063	0.9222	**0.9341**	0.9253	0.9120
256×256	21.4	0.9045	0.8820	0.4061	0.9279	**0.9331**	0.9277
512×512	25.5	0.9033	0.9061	0.7923	0.7688	0.9251	**0.9314**

consuming. In order to improve the efficiency of the algorithm, in our implementation the image is partitioned into blocks, then the mean value of the obtained quality indices extracted from each block is taken as the overall image quality. The smaller the block size, the less the time involved in each calculating SVD, but more blocks implies more transforms. Hence the size of the blocks must be considered with respect to both SVD complexity as a function of block size and with respect to block cardinality. At the same time, the performance of the algorithm is also affected by block size. We performed a simulation using 150 images from the CSIQ database to obtain runtimes and performance for different block sizes and values of α, as shown in Table 2. Since the shortest time incurred was on 128×128 blocks, the performance of the exemplar algorithm was the best; thus we fixed the block size to be 128×128 in the next experiment.

4.3. C. Determination of Parameters α and β

The values of parameters α and β must be determined in (2) and (9). We applied the parameter values 0.5, 3, 7, 11, 15, 19 and tested Q_{area} and $Q_{exponent}$ on the LIVE IQA database. The results are shown in Tables 3 and 4.

From Tables 3 and 4, it can be seen that for JPEG, JP2K, Blur and FF distorted categories, the performance of Q_{area} is best when the value of α equals 15; when $\beta=7$, the best results of $Q_{exponent}$ are achieved. But white noise type is an exception, when the values of α and β are 0.5, both Q_{area} and $Q_{exponent}$ reach the optimal performance. So in the following experiment, for white noise distortion alone, the values of α and β are set to 0.5; for the other single and all distortion, α is set to 15 for calculating Q_{area}, and β is set to 7 for calculating $Q_{exponent}$.

Table 3
Performance of Q_{area} using different values of α on the LIVE databse.

Measure		$\alpha=0.5$	$\alpha=3$	$\alpha=7$	$\alpha=11$	$\boldsymbol{\alpha=15}$	$\alpha=19$
SROCC	WN	**0.9723**	0.9661	0.9450	0.9165	0.8819	0.8407
	JPEG	0.2640	0.8194	0.9061	0.9376	**0.9514**	0.9548
	JP2K	0.8612	0.7061	0.9000	0.9236	**0.9232**	0.9192
	Blur	0.9413	0.8477	0.9323	0.9441	**0.9412**	0.9379
	FF	0.8616	0.7812	0.8139	0.8540	**0.8587**	0.8551

Table 4
Performance of $Q_{exponent}$ using different values of β on the LIVE database.

Measure		$\beta=0.5$	$\beta=3$	$\boldsymbol{\beta=7}$	$\beta=11$	$\beta=15$	$\beta=19$
SROCC	WN	**0.9537**	0.9428	0.9208	0.8977	0.8579	0.8094
	JPEG	0.4820	0.9168	**0.9424**	0.9224	0.9043	0.8860
	JP2K	0.7923	0.5060	**0.9255**	0.8780	0.8447	0.8163
	Blur	0.9195	0.8240	**0.9077**	0.8919	0.8554	0.8395
	FF	0.8251	0.7190	**0.8047**	0.8277	0.8272	0.8176

4.4. D. Distortion identification

Since the values of α and β for white noise and other distortions are different, then to make the Q_{area} and $Q_{exponent}$ indices applicable to diverse distorted images, we must classify a given image into noise or non-noise distortion categories. In [27] the authors propose a new noise variance estimation method based on principal component analysis of image blocks. We use a threshold of noise variance for classifying noise and non-noise images. The results of classification on five databases are shown in Table 5, it can be seen that the noise and non-noise distortion are classified completely when we set the threshold to 1.6. Thus, we use the first stage ("distortion identification") of the Q_{area} and $Q_{exponent}$ algorithms. This stage does not utilize human opinion scores.

4.5. E. Test on the LIVE database

Firstly, we tested the Q_{area} and $Q_{exponent}$ indices on the LIVE2 IQA database, which consists of 779 distorted images from 29 different reference images. There are five distortions —JPEG2000 (JP2K), JPEG (JPEG), Gaussian Blur (Blur), White Noise (WN) and Fast fading noise (FF)—along with the associated DMOS, which represent human judgments of image quality. Their performance was tested and compared with two state-of-the-arts representative NR IQA metrics, NIQE [16] and NRQI [17], and two classical FR IQA metrics, SSIM [28] and PSNR. For NIQE [16] and SSIM, we used the

Table 6
Performance of Q_{area} on the LIVE database.

Measure		Q_{area}	$Q_{exponent}$	NIQE	NRQI	SSIM	PSNR
SROCC	WN	**0.9723**	0.9537	**0.9718**	0.9357	0.9635	0.9410
	JPEG	**0.9514**	**0.9424**	0.9422	0.8715	0.9466	0.8831
	JP2K	**0.9232**	**0.9255**	0.9187	0.8074	0.9389	0.8646
	Blur	**0.9412**	0.9077	**0.9329**	0.8562	0.9046	0.7515
	FF	**0.8587**	0.8047	**0.8639**	0.8181	0.9393	0.8736
	ALL	**0.9006**	0.8362	**0.8756**	0.8263	0.9129	0.8636
CC	WN	**0.9717**	0.9579	**0.9773**	0.9482	0.9824	0.9173
	JPEG	**0.9506**	0.9429	**0.9526**	0.8911	0.9462	0.9029
	JP2K	**0.9310**	**0.9359**	0.9264	0.8126	0.9405	0.8762
	Blur	**0.9371**	0.9176	**0.9447**	0.8765	0.9004	0.7801
	FF	**0.8574**	0.8101	**0.8804**	0.8435	0.9514	0.8795
	ALL	**0.8953**	0.8523	**0.8815**	0.8350	0.9066	0.8592

Table 5
The range of noise variance values on the five databases.

Database	JPEG	JP2K	Blur	FF	White noise	Hi-noise	Col-noise
LIVE2	0–0.62	0–1.50	0–1.44	0–0.98	1.82–73.15	–	–
TID2008	0–0.48	0–0.66	0–0.49	–	2.89–15.50	2.09–24.14	1.90–7.88
CSIQ	0–1.48	0–1.08	0–1.11	–	1.68–17.02	–	–
TOYAMA	0–1.58	0–1.52	–	–	–	–	–
IVC	0	0	0–0.41	–	–	–	–

implementation provided by the author, which is available online at http://live.ece.utexas.edu/research/Quality/index.htm. For NRQI and PSNR, we implemented them by ourselves. The experimental results are shown in Table 6.

From Table 6, it can be seen that the indices Q_{area} and $Q_{exponent}$ correlate well with human DMOS, and that the performance of the index Q_{area} is a little better than that of $Q_{exponent}$. On the Blur, JP2K, JPEG and WN distortion categories, the Q_{area} index delivers better performance than NIQE, NRQI and PSNR. But on the FF and ALL categories its results are a little inferior to that of NIQE and SSIM.

We also created scatter plots of the scores of the Q_{area} index against DMOS on the five individual and all distorted categories of LIVE databases, as shown in Fig. 5(a)–(f), which further suggests that Q_{area} index is consistent with human subjective judgments.

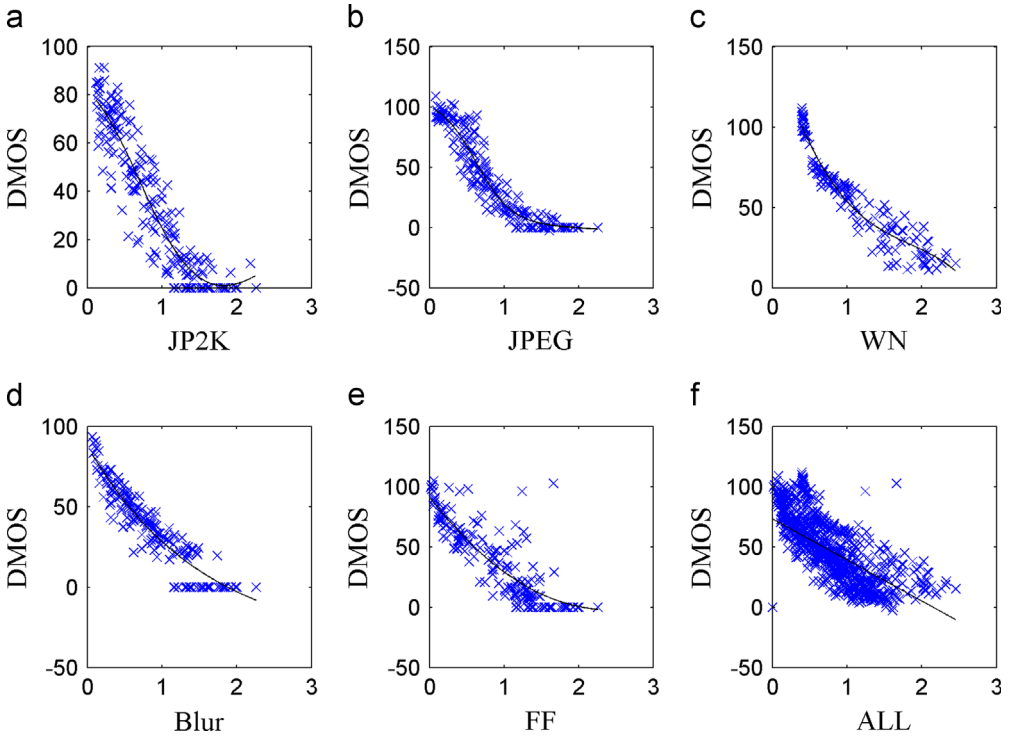

Fig. 5. Q_{area} index against difference mean opinion scores (DMOS) on LIVE individual distortion databases. (a) JP2K; (b) JPEG; (c) WN; (d) Blur; (e) FF and (f) all.

Table 7
SROCC comparison of several IQA metrics.

Database		Q_{area}	$Q_{exponent}$	NIQE	NRQI	SSIM	PSNR
TID2008	WN	**0.8040**	0.7532	**0.7797**	0.6082	0.7965	0.9148
	WN-color	**0.7458**	**0.6029**	0.6012	0.5869	0.8075	0.9028
	high-fre-noise	**0.9278**	**0.9234**	0.8539	0.8234	0.8451	0.9273
	Blur	0.8261	**0.8560**	**0.9092**	0.7812	0.9386	0.8684
	JPEG	**0.8929**	**0.8664**	0.8609	0.7490	0.8989	0.8717
	JP2K	**0.9364**	0.7715	**0.8934**	0.8765	0.8875	0.8132
CSIQ	WN	**0.8888**	0.8043	**0.8098**	0.8034	0.9255	0.9363
	JPEG	**0.9378**	**0.9382**	0.8826	0.8568	0.9222	0.8882
	JP2K	**0.9120**	0.8995	**0.9065**	0.8976	0.9207	0.9362
	Blur	**0.9253**	0.8891	**0.8944**	0.8743	0.9245	0.9291
TOYAMA	JPEG	**0.8806**	**0.8443**	0.8007	0.8035	0.7388	0.8523
	JP2K	0.7772	**0.8179**	**0.8676**	0.7865	0.9221	0.8346
IVC	JPEG	**0.8813**	**0.8523**	0.8271	0.8342	0.7975	0.6637
	JP2K	**0.9226**	**0.9225**	0.8507	0.8721	0.8488	0.8500
	Blur	**0.8871**	0.8577	**0.8638**	0.8756	0.8691	0.8051

Table 8
CC comparison of several IQA metrics.

Database		Q_{area}	$Q_{exponent}$	NIQE	NRQI	SSIM	PSNR
TID2008	WN	**0.7838**	0.7356	**0.7797**	0.6134	0.7913	0.9378
	WN-color	**0.7115**	**0.6268**	0.6134	0.6291	0.8162	0.9273
	High-fre-noise	**0.9428**	**0.9385**	0.8539	0.8342	0.8574	0.9718
	Blur	0.8444	**0.8573**	**0.9092**	0.8046	0.9342	0.8736
	JPEG	**0.9193**	**0.8766**	0.8609	0.7634	0.9143	0.8703
	JP2K	**0.9370**	0.7695	**0.8934**	0.8653	0.8841	0.8759
CSIQ	WN	**0.8951**	**0.8107**	0.8098	0.8012	0.9256	0.9532
	JPEG	**0.9550**	**0.9382**	0.8826	0.8512	0.9420	0.8906
	JP2K	**0.9283**	0.8995	**0.9065**	0.9065	0.9236	0.9468
	Blur	**0.9424**	**0.9151**	0.8944	0.8882	0.8504	0.9252
TOYAMA	JPEG	**0.8846**	**0.8384**	0.8007	0.8131	0.7566	0.8643
	JP2K	0.8019	**0.8351**	**0.8676**	0.7735	0.9357	0.8267
IVC	JPEG	**0.8718**	**0.8526**	0.8271	0.8547	0.8252	0.6678
	JP2K	**0.9186**	**0.9175**	0.85073	0.8846	0.8630	0.8476
	Blur	**0.8674**	**0.9302**	0.8638	0.8775	0.9177	0.8959

4.6. F. Test on other IQA database

We also examined the performance of the Q_{area} and $Q_{exponent}$ on the other four open databases, including TID2008, CSIQ, TOYAMA and IVC. The experimental results are summarized in Tables 7 and 8.

From Tables 7 and 8, it can be concluded the Q_{area} index is a little better than the $Q_{exponent}$ index for most distortion categories. In most cases, both Q_{area} and $Q_{exponent}$ outperform the up-to-date blind IQA index NIQE, which is the best completely blind index in the current reported reference. Moreover, for some distorted categories, which the NIQE index loses effect in, such as "WN-color" and "high-fre-noise" artifacts from the TID2008 database; our proposed Q_{area} index also delivers quality pridictions that are highly consistent with human subjective judgments.

5. Conclusion

In this paper, the reciprocal singular value curves of natural images, and their relationships with image quality are analyzed, resulting in two blind image quality assessment metrics based on the area and exponent of reciprocal singular value curves. The comparison of both proposed indices with blind IQA metrics on five open database show they have an impressive consistency with human subjective perception and are competitive with state-of-the-art blind IQA metrics. They even outperform standard full reference algorithms for some distortions. The proposed Q_{area} and $Q_{exponent}$ indices have the following advantages. (1) Simple mathematical expression leads to low computational complexity; (2) they can be applied to more distorted categories, such as "High frequency noise," and "WN-color." How to extend these indices to evaluate the quality of an image with mixed multi-distortions will be future work.

Acknowledgments

This research is supported in part by the National Natural Science Foundation of China (No. 61170120), Program for New Century Excellent Talents in University (NCET-12–0881), the Fundamental Research Funds for the Central Universities (JUSRP51410B), the 111 Project (B12018), the Natural Science Foundation of Jiangsu Province (No. BK2011147). A. C. Bovik was supported by the U.S. National Science Foundation under Grant IIS-1116656.

References

[1] Z. Wang, A.C. Bovik, Modern Image Quality Assessment, Morgan and Claypool Publishing Company, USA, New York, 2006.
[2] W. Lin, C.C. Jay Kuo, Perceptual visual quality metrics: a survey, J. Vis. Commun. Image Represent. 22 (4) (2011) 297–312.
[3] R. Ferzli, L.J Karam, A no-reference objective image sharpness metric based on the notion of Just Noticeable Blur (JNB), IEEE Trans. Image Process. 18 (4) (2009) 717–728.
[4] R. Hassen, Z. Wang, and M. Salama, No-reference image sharpness assessment based on local phase coherence measurement, IEEE International Conference on Acoustics Speech and Signal Processing (ICASSP10), Dallas, 2010, vol. 1, pp. 2434–2437.
[5] N.D. Narvekar, L.J. Karam, A no-reference image Blur metric based on the cumulative probability of Blur detection (CPBD), IEEE Trans. Image Process. 20 (9) (2011) 2678–2683.
[6] C.F. Li, W. Yuan, A.C. Bovik, X.J. Wu, No-reference Blur index using Blur comparisons, Electron. Lett. 47 (17) (2011) 962–963.
[7] H.R. Sheikh, A.C. Bovik, L. Cormack, No-reference quality assessment using natural scene statistics: JPEG2000, IEEE Trans. Image Process. 14 (11) (2005) 1918–1927.
[8] P. Marziliano, F. Dufaux, S. Winkler, T. Ebrahimi, Perceptual blur and ringing metrics: application to JPEG2000, Signal Process.: Image Commun. 19 (2) (2004) 163–172.
[9] C. Li, A.C. Bovik, X. Wu, Blind image quality assessment using a general regression neural network, IEEE Trans. Neural Netw. 22 (5) (2011) 793–799.
[10] A.K. Moorthy, A.C. Bovik, Blind image quality assessment: from scene statistics to perceptual quality, IEEE Trans. Image Process. 20 (12) (2011) 3350–3364.
[11] P. Ye, J. Kumar, L. Kang, and D. Doermann. Unsupervised feature learning framework for no-reference image quality assessment. In CVPR, 2012.

[12] M.A. Saad, A.C. Bovik, C. Charrier, Model-based blind image quality assessment: a natural scene statistics approach in the DCT domain, IEEE Trans. Image Process. 21 (8) (2012) 3339–3352.
[13] A. Mittal, A.K. Moorthy, A.C. Bovik, No-reference image quality assessment in the spatial domain (Dec.), IEEE Trans. Image Process. 21 (12) (2012) 4695–4708.
[14] A.K. Moorthy, A.C. Bovik, A two-step framework for constructing blind image quality indices (Dec.), IEEE Signal Process. Lett. 17 (5) (2010) 513–516.
[15] A. Mittal, G.S. Muralidhar, A.C. Bovik, Blind image quality assessment without human training using latent quality factors (Dec.), IEEE Signal Process. Lett. 19 (2) (2012) 75–78.
[16] A. Mittal, G.S. Muralidhar, A.C. Bovik, Making a 'completely blind' image quality analyzer, IEEE Signal Process. Lett. 20 (3) (2013) 209–212.
[17] W. Xue, L. Zhang, X. Mou, Learning without Human Scores for Blind Image Quality Assessment, In CVPR, 2013.
[18] C.F. Li, Y. Ju, A.C. Bovik, X.J. Wu, Q.B. Sang, No-training, no-reference image quality index using perceptual features, Opt. Eng. 52 (5) (2013) 057003-1-6.
[19] A. Shnayderman, A. Gusev, A.M. Eskicioglu, An SVD-based grayscale image quality measure for local and global assessment, IEEE Trans. Image Process. 15 (2) (2006) 422–429.
[20] M. Narwaria, and W. Lin, Objective image quality assessment with singular value decomposition, Fifth International Workshop on Video Processing and Quality Metrics for Consumer Electronics (VPQM), 2010.
[21] E.C. Larson and D.M. Chandler, Categorical Image Quality (CSIQ) database 2009 [Online]. Available: ⟨http://vision.okstate.edu/csiq⟩.
[22] H.R. Sheikh, K. Seshadrinathan, et al., Image and Video Quality Assessment Research at LIVE 2004 [Online]. Available: ⟨http://live.ece.utexas.edu/research/quality⟩.
[23] N. Ponomarenko, V. Lukin, A. Zelensky, et al., TID2008—a database for evaluation of full-reference visual quality assessment metrics, Adv. Mod. Radioelectron. 10 (4) (2009) 30–45.
[24] A. Ninassi, P. Le Callet, and F. Autrusseau, Subjective Quality Assessment- IVC Database 2005 [Online]. Available: ⟨http://www2.irccyn.ecnantes.fr/ivcdb⟩.
[25] Y. Horita, K. Shibata, Y. Kawayoke, and Z.M.P. Sazzad, MICT Image Quality Evaluation Database 2000 [Online]. Available: ⟨http://mict.eng.u-toyama.ac.jp/mict/index2.html⟩.
[26] A. Ciancio, A.L.N.T. Da Costa, et al., No-reference blur assessment of digital pictures based on multi-feature classifiers, IEEE Trans. Image Process. 20 (1) (2011) 64–75.
[27] S. Pyatykh, J. Hesser, L. Zheng, Image noise level estimation by principal component analysis, IEEE Trans. Image Process. 22 (12) (2012) 5226–5237.
[28] Z. Wang, A.C. Bovik, H.R. Sheikh, E.P. Simoncelli, Image quality assessment: from error visibility to structural similarity, IEEE Trans. Image Process. 13 (4) (2004) 600–612.